RHEOLOGICAL PROPERTIES OF BITUMENS MODIFIED WITH SELECTED ULTRA-FINE FILLERS

Salah E. Zoorob[1], *Georges A J Mturi*[2], *Joseph Anochie Boateng*[2]
[1]*Coventry University, Dept. of Built Environment, Coventry, UK*
[2]*Council for Scientific & Industrial Research, Pretoria, South Africa*

ABSTRACT

This paper highlights results of a laboratory investigation into the rheological properties of a number of straight run bitumens compared to a proprietary SBS modified bitumen and to a bitumen modified with selected micro (calcium carbonate) and nano (clay) fine fillers. The fillers, which were incorporated into the bitumen using high shear blending, were specifically selected for their high temperature storage stability. The ability of the fillers to impart enhanced rheological performance on the resultant binders at high temperatures was assessed using two primary modes of DSR testing, i.e. dynamic oscillatory testing and multiple stress creep recovery (MSCR) tests. MSCR tests were conducted at pre-determined target viscosities and at a pre-determined test temperature. The effect of utilizing constant shear stress versus constant shear rate data on the Arrhenius activation energy values for viscous flow was investigated. The paper highlights the benefits of SBS modification, and the potential for improving the resistance to high temperature dynamic creep using two very different ultra-fine filler types.

Keywords: bitumen rheology, micro and nano-fillers, Multiple Stress Creep Recovery

1. Introduction

The resistance of asphalt mixtures to permanent deformation is related to the stiffness of bitumen, mix volumetrics, and the bonding interaction between bitumen and aggregate. Bitumens are approximately 20 times more temperature dependent than many polymeric materials. Over most of the range of interest in paving applications, the rate of change of complex modulus (G*) with respect to temperature ranges from 15 to 25 percent/°C [10].

Selecting a stiffer grade of bitumen, polymer modification and more unusually blending with ultra-fine fillers, are three viable means of improving the resistance of bitumen to high temperature creep loading. The following investigation starts by assessing and contrasting conventional temperature dependency of a straight run 40/50 pen versus a proprietary SBS modified bitumen viscosities based on the Arrhenius relation. This is followed by experimental trials using the low shear viscosity (LSV) concept and multiple stress creep recovery (MSCR) tests at pre-determined viscosities on the same 40/50 pen and SBS-modified bitumens in addition to a straight run 20/30 pen.

In the final stage of this paper, the MSCR mode of loading at a pre-determined test tempearature was adopted as the preferred test method. In addition to the aforementioned bitumens, a number of storage stable fine filler-bitumen blends (based on a calcium carbonate micro-filler and an organic modified clay nano-filler) were formulated and assessed using frequency sweeps and black diagrams. The best performing micro and nano filler-bitumen formulations were finally MSCR tested and the results compared directly to the performance of the straight run and SBS modified bitumens.

2. Temperature Dependency of Viscosity based on the Arrhenius Relation

Viscous flow in any liquid can be regarded as a thermally activated rate process where atoms, molecules or groups of molecules must overcome an energy barrier to move to an adjacent vacant site or "hole". When a liquid flows, layers of liquid molecules slide over each other, where intermolecular forces oppose the motion and cause resistance to flow. This results in an activation energy barrier for viscous flow that must be overcome. As temperature increases, the fraction of molecules with the necessary activation energy increases and the energy barrier is easier to overcome [16].

Presently, there are two commonly used expressions to evaluate the temperature dependency of viscosity, one based on the free-volume concepts, namely the Williams, Landel & Ferry (W-L-F) equation and the second, of the Arrhenius type, based on the absolute theory of rate processes as derived by Eyring. For temperatures closer to T_g, it is recommended that the W-L-F relation is used (Eq. 1). The Arrhenius relation (Eq. 2) is most commonly used for low-viscosity liquids and polymer melts in the range $[T > (T_g + 100K)]$, where T_g = glass transition temperature [16].

W-L-F equation $$\log \frac{\eta}{\eta_s} = \frac{C_1(T-T_s)}{C_2+(T-T_s)} \qquad \text{...(1)}$$

where: η and η_s = viscosities at temperatures T and T_s respectively, C_1 and C_2 are constants, T_s = the standard reference temperature taken as $T_g + 50°K$, where T_g = glass transition temperature.

Arrhenius-Eyring Equation $$\eta(T) = Ae^{(E_f)/(RT)} \quad \text{or} \quad \ln \eta = (E_f)/(RT) + \ln A \qquad \text{...(2)}$$

where: η = viscosity of bitumen at temperature T, T = temperature in Kelvin, E_f = activation energy for viscous flow (kJ/mol), R = universal gas constant [8.314×10^{-3} kJ/(mol.K)]. E_f describes the energy needed for the molecules to exceed the liquid-specific energy barrier (potential energy), A = frequency term depending on the entropy of activation for flow. Using this energy the molecules are able to move against the internal flow resistance which is caused by the friction between the neighbouring molecules.

In general, using the Arrhenius treatment, the following also holds for the viscosity-temperature shift factor a_T. The dimensionless factor a_T is the ratio of the viscosity values at the temperature T to the value at the reference temperature T_{ref}.

$$a_T = \left[\eta(T) \div \eta(T_{ref})\right] \qquad a_T = \exp\left[\frac{E_f}{R}\left(\frac{1}{T} - \frac{1}{T_{ref}}\right)\right] \qquad \text{...(3)}$$

By calculating shift factor using a reliable set of viscosity-temperature data measurements it becomes possible to determine the viscosity values at temperatures for which no measurements are available. Additionally, by plotting η (on a natural log scale) versus 1/T (on a linear scale), the so-called Arrhenius curve (temperature dependent behaviour) is produced.

2.1 Temperature dependency of bitumen derived from conventional test methods

Viscosity–temperature relationships have traditionally been constructed by measuring penetration, softening point and Brookfield viscosity at a range of temperatures. At the Softening point temperature, the viscosity of an unaged non-modified bitumen can be assumed to be equal to 13000 Poise. Penetration data can also be converted to viscosity using the following equation [9]:

$$\text{Log } \eta = 10.5012 - 2.2601 \log(pen) + 0.00389 \log(pen)^2 \qquad \text{...(4)}$$

where: η = bitumen viscosity (poise), pen = penetration for 100g & 5sec loading (mm/10).

Viscosity values can also be obtained at a range of temperatures using a dynamic shear rheometer (DSR) by conducting a temperature sweep typically at a fixed frequency of 1.59Hz (10 rad/s), as an example using the following equation [9]:

$$\eta = \frac{G^*}{10}\left(\frac{1}{\sin\delta}\right)^{4.8628} \qquad \text{...(5)}$$

where: η = bitumen viscosity (cP), G^* = bitumen complex shear modulus at 10 rad/s (Pa), δ = phase angle (degrees).

An example of test data generated from applying the aforementioned test methods on a straight run 40/50 pen bitumen compared to proprietary styrene-butadiene-styrene (SBS) block copolymer modified bitumen (classified as PG 64) are shown in Fig. 1. In Fig. 1, the measured data points for the 40/50 pen were; softening point (symbol = **Δ**), Brookfield viscosities at; 60, 70, 80, 110, 135, 165°C (symbol = **x**), and DSR runs at 1.59Hz conducted at 20, 40, 55 and 70°C (symbol = □). For the DSR runs at the standard 1.59Hz, the G* output were converted to viscosity values using (Eq. 5) before plotting them in Fig. 1.

Activation energy for flow E_f is obtained by multiplying the slope of the line in Fig. 1 by the universal gas constant R. A typical example of an E_f value for the 40/50 pen bitumen tested as part of this investigation was around 77 kJ/mol (18.48 kcal/mol).

With respect to the SBS modified bitumen, the slope of the line in Fig. 1 at high temperatures is not too dissimilar to that of the pen grade bitumen. Nonetheless, it was not possible to measure Brookfield viscosities below about 80°C, and even the value determined at 80°C had to be discarded due to predominant shear thinning behaviour [9], equally the softening point determination had to be discarded for unreliability.

The complexity of the viscosity of SBS block copolymers are a manifestation of the existing two-phase structured system. As the temperature is raised, only one of the domains of the two-phase system melts, but the system is able to flow as a whole due to the fluidity created by one of the domains despite the fact that the two domains are not compatible. As the temperature rises, a stage is reached when both domains become fluid and the additional resistance to flow due to the presence of the unmelted domain is removed. In the case of pure SBS polymer, between 110-150°C, the activation energy E_1 reported in the literature has a value of 28.7 kcal/mole which is not too different from the activation energy for homopolystyrene (E_f = 25.5 kcal/mole), whereas in the temperature range between 150 to 210°C, the activation energy tends to that of polybutadiene (E_f = 4.5 to 7.9 kcal/mol) and takes a lower value of E_2 = 10.0 kcal/mole [12].

Considering the Softening point, Brookfield and DSR (1.59Hz) viscosity derived data, the viscosity-temperature profile of the two binders as shown in Fig. 1 indicates that to ensure the adequacy of the Arrhenius relationship, and consequently the shift factor a_T, only viscosity values below around 70 Pa.s must be considered, otherwise a linear relationship is not valid. These findings add doubt to the usefulness of the Arrhenius treatment of bitumen viscosity data across the entire temperature range (from production to service) when applied to road surfacing asphalts.

2.2 Effect of shear stress on Arrhenius relation

Theoretically, the Arrhenius relation described earlier “only” applies to thermo-rheologicaly simple materials. In other words, materials which do not undergo a change in the structural character in the observed temperature range, henceforth they do not change from the “sol state” to a “gel state” or vice versa. Interestingly, it has been suggested that in the non-Newtonian (shear-thinning) region of polymer flow, a clear differentiation between E at a constant shear stress and E at a constant shear rate must be done [12, 16]. Thus;

$$E_\tau = R\left[\frac{\ln\eta}{(1/T)}\right]_\tau \qquad \text{...(6)} \qquad\qquad E_{\dot\gamma} = R\left[\frac{\ln\eta}{(1/T)}\right]_{\dot\gamma} \qquad \text{...(7)}$$

where; $E_\tau > E_{\dot\gamma}$ for shear thinning non-Newtonian viscosity.

The literature also reports that for a variety of polymers, E_τ remains constant over a broad range of temperature and shear-stress (from low-shear Newtonian range up to shear stresses of ≈ 10^5 Pa, well within the non-Newtonian region), while $E_{\dot\gamma}$ does not. From a fundamental viewpoint, constant shear rate “activation energies” are incorrect because the Arrhenius equation is a rate equation, and hence holding the rate process constant would make data treatment meaningless [12].

To explore the effect of shear stress on the Arrhenius relationship, further DSR temperature sweeps were conducted at a much lower frequency of 0.01Hz covering the temperature range from 40°C to 58°C (symbol = **Δ**) and 40°C to 53°C for the 40/50 pen (symbol = **o**) as shown in Fig. 2. By reducing the frequency (or time of loading) at any one test temperature, one is clearly reducing the magnitude of shear stress. The 40/50 pen 0.01Hz data points fall nicely within the expected trend line, whereas the SBS 0.01Hz data points clearly do not comply with the results obtained from the three tests described earlier and form a separate grouping. In summary, these results cast a dark shadow over the validity of the Arrhenius relationship when testing materials that are thermo-rheologically not simple.

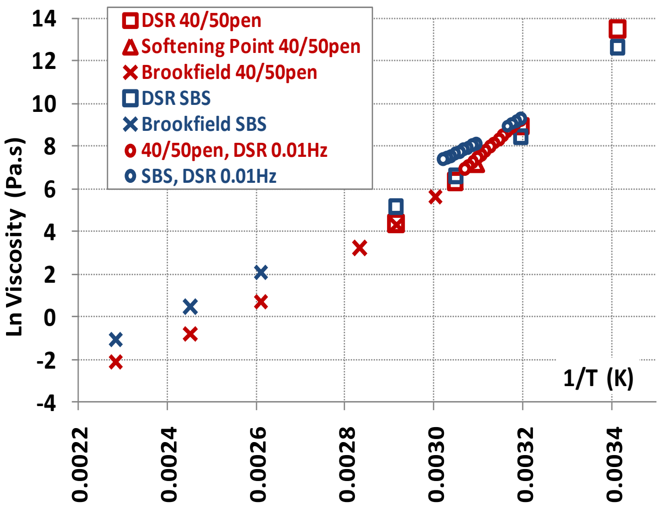

Figure 1: Arrhenius plot for a 40/50pen compared to an SBS modified binder.

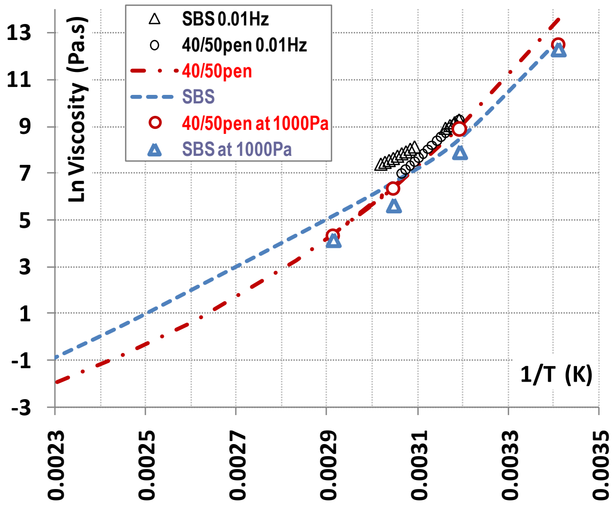

Figure 2: Arrhenius plot for a 40/50pen compared to SBS bitumen incorporating tests at 0.01Hz and data at 1000Pa.

3. Quantifying High Temperature Creep using LSV and MSCR Tests at pre-set Target Viscosities

For bitumens where it is possible to experimentally define Zero-shear viscosity (ZSV) (i.e. limiting value of shear rate-dependent viscosity η_0 at an "infinitely low" shear rate), good correlations between asphalt mix rutting and η_0 of the bitumen have been shown to exist. Unfortunately, the time required to attain steady state flow during static creep tests depends on the type of bitumen being analysed and spans from a few minutes for a conventional pen. grade bitumen to in excess of 12 hours for elastomer-rich phase polymer modified bitumen exhibiting delayed elasticity [2, 5, 14].

This was the driver for the introduction of the low shear viscosity (LSV) concept, defined as the dynamic viscosity at a shear stress or shear rate close to zero. Instead of measuring LSV at a fixed temperature, it has been proposed to measure the temperature at which LSV attains a fixed value. Furthermore, a requirement of a minimum viscosity of 2 kPa.s has been recommended for viscosity tests at very low shear rates (approaching zero) to ensure a sufficient contribution of the bitumen to rut resistance in an asphalt pavement under heavy duty traffic at high in-service temperatures [4, 15].

In this part of the investigation, the same two bitumens described earlier (i.e. 40/50 pen and SBS modified bitumen) were supplemented with a straight run 20/30 pen and were all tested in the unaged state using the LSV concept in accordance with prCEN/TS-15324:2006 guidelines. The LSV test protocol adopted involves a temperature sweep (whilst maintaining strain within the Linear Viscoelastic - LVE range) carried out in 1°C increments at 0.01 Hz. A plot of log complex viscosity versus temperature as shown in Fig. 3 is next used to determine the temperature (referred to as an equiviscous temperature EVT) at which the viscosity value of each bitumen type becomes equal to 2 kPa.s. Once EVT is identified for a particular bitumen sample, a frequency sweep is subsequently conducted at the EVT temperature at progressively lower shear rates (e.g. covering the range from 1 Hz down to 0.003 Hz), as shown in Fig. 4.

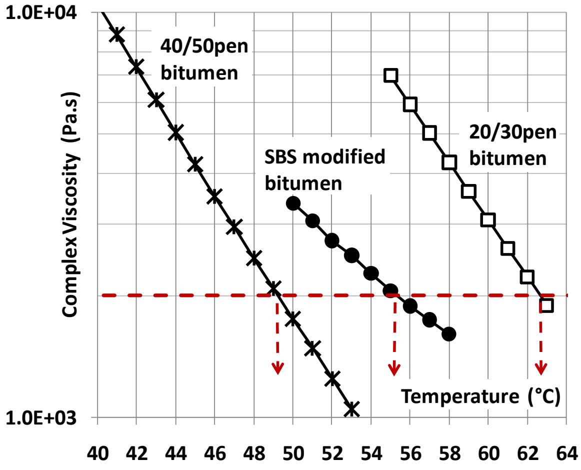

Figure 3: Temperature sweeps at 0.01Hz to obtain an equi-viscous temperature values at $\eta^* = 2$kPa.s

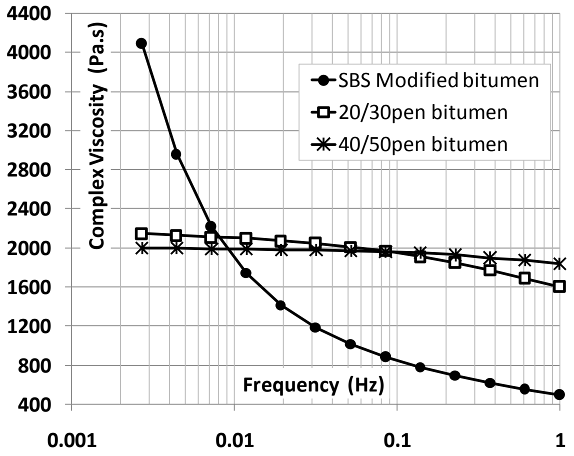

Figure 4: Complex viscosity data obtained from frequency sweeps at equi-viscous temperature EVT.

In theory, using a plot as in Fig. 4 would allow curve fitting to be used to project viscosity values to shear rates approaching zero (e.g. 0.0001 Hz). Fig. 4 shows clearly that it is feasible to apply rheologic fitting functions such as the Cross or Carreau models for straight run bitumens (in this example a regular 40/50pen is contrasted with a harder 20/30pen grade). On the other hand, for an elastomer (SBS) modified bitumen, the concepts of zero or low shear viscosity are not readily applicable as no viscosity plateau can be observed at very low shear rates. The viscosity profile of the SBS bitumen is in line with what is expected from testing a cross linked polymer [19].

In response to the difficulties faced when applying ZSV and LSV concepts to the SBS modified binder tested in this investigation it was decided to explore another more recent high temperature bitumen test characterisation tool, namely the multiple stress creep recovery test (MSCR) [3, 13]. The most commonly accepted MSCR test procedure [13] uses a 1 second creep loading with 9 second recovery over the multiple stress levels of 25, 50, 100, 200, 400, 800, 1600, 3200, 6400, 12800 and 25600 Pa, applying 10 cycles at each stress level. The average non-recovered strain for the 10 creep and recovery cycles is then divided by the applied stress for those cycles yielding the non-recoverable compliance J_{nr}.

In this investigation, two test temperatures were selected for each bitumen type as shown in Table 1. The first temperature was selected to be in line with the traditional ($G^*/\sin\delta$ = 1kPa) criterion for unaged bitumens [10]. The second temperature was selected to be equal to the EVT value (at η^* = 2 kPa.s, as described earlier in Fig. 3).

Table 1: MSCR test temperatures adopted in this investigation

	40/50 pen	20/30 pen	SBS
SHRP ($G^*/\sin\delta$) test temperature (°C), tested at 10 rad/s	67	83	73
EVT test temperature (°C), tested at 0.01Hz	49.2	62.4	55.3

Fig. 5 compares the strain response during 10 load-unload pulses of an MSCR test for all three bitumen types at an arbitrarily selected stress level of 800 Pa. In this example all the bitumens were tested at their ($G^*/\sin\delta$ = 1 kPa) criterion. The figure highlights the large magnitudes of strain recoveries (delayed elastic response) displayed by the SBS modified bitumen (saw tooth shape response) in comparison to the non-modified samples (very little recovery, staircase response). It is equally interesting to note the comparatively low cumulative strain values of the SBS modified bitumen in relation to the other two straight run samples.

Fig. 6 shows a plot of the percentage non-recoverable compliance (J_{nr}) versus applied stress for all three bitumen samples at all the test temperatures described earlier in Table 1. The lower 3 lines in Fig. 6 show that at the EVT test temperatures, all the bitumen types performed very well with consistent compliance. On the other hand, when the test temperatures were raised to match the $G^*/\sin\delta$ criterion, marked differences between the three bitumen types were observed. In this case, as the stress level increased in the MSCR test, the sensitivity to stress became apparent and differences in bitumen response (inflection point) were evident.

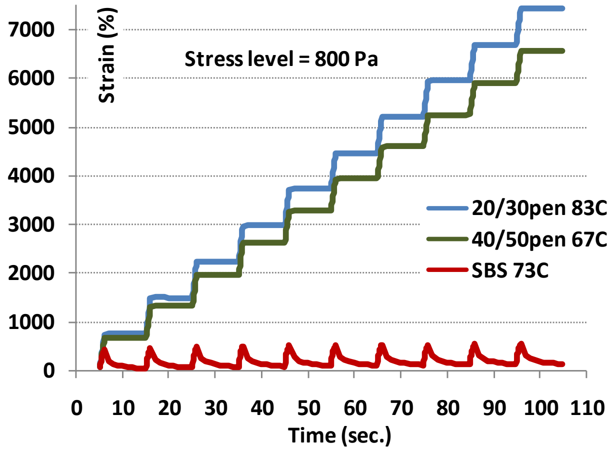

Figure 5: An example of MSCR test loading results at a stress level of 800 Pa.

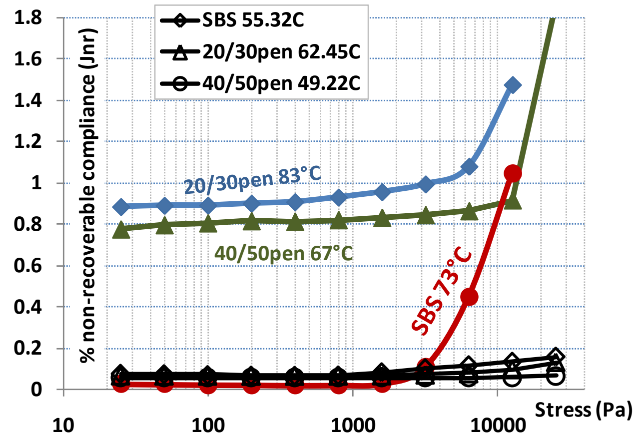

Figure 6: Comparison of MSCR J_{nr} values for the three bitumens investigated.

Despite the fact that the SBS modified bitumen had the lowest J_{nr} values, at stress levels in excess of approximately 3000 Pa, the sample changed from being the most resistant to deformation to the worst. Normally, pen grade bitumens exhibit shear thinning, the extent of which varies based on the base bitumen and the modification type. It is possible that the stress dependency of polymer modified bitumens may be due to, at least in part, the non-linear response of polymers to high strain.

The G*/sinδ and the EVT criterion already creates a level of complexity as bitumens have to be characterised at different test temperatures. Analysing stress sensitivity has introduced further complications to the already difficult task of predicting bitumens' performance. This is especially so since the actual stress profile of the bitumen phase in an in-situ asphalt composite under traffic loading cannot be obtained by simple means. One possible way forward to simplify the bitumen comparison exercise would be to conduct all MSCR tests at the actual expected maximum pavement temperature. In the following section further MSCR tests were thus conducted on an expanded range of bitumen types at a fixed high test temperature value in order to facilitate better analysis of stress sensitivity.

4. MSCR Testing at Pre-Set Temperatures

One of the key outcomes of Part 3 of this investigation was that MSCR testing at pre-determined viscosity targets, (i.e. G*/sinδ > 1kPa or the 2 kPa.s targets), resulted in markedly different test temperatures for the various bitumen types and grades. It was thus decided to focus Part 4 of the investigation on MSCR testing and comparison of binder performance at a pre-determined temperature value. To this end, the same three binders as used in Parts 2 & 3 were redeployed, but additionally a number of filler-bitumen systems were manufactured and introduced as part of this investigation as described below.

4.1 Additional binders introduced for Part 4 testing

In addition to the 20/30 pen, 40/50 pen and the SBS modified bitumen used in Parts 2 & 3 of this investigation, a straight run 60/70 pen was introduced having a SHRP PG grading (G*/sinδ ≥ 1 kPa) measured at 64°C. Fig. 7 compares the complex viscosity versus frequency sweep curves of the 60/70 pen bitumen to the aforementioned bitumens.

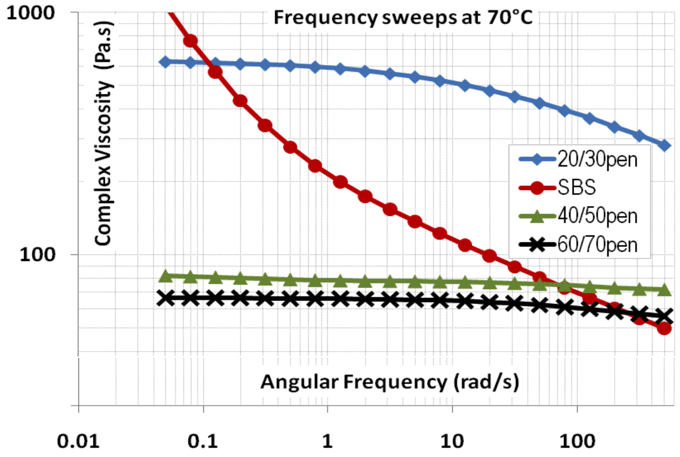

Figure 7: DSR complex viscosity versus frequency trend lines for unfilled-bitumens

A growing number of recent publications have highlighted the advantages of intimately blending micro-fine or nano-fine fillers with bitumen. For example, the exfoliated structure of organo-montmorillonite (OMMT) nano-composites blended with bitumen was shown to improve both thermo-oxidative and UV ageing properties in comparison to the virgin bitumen [17]. Similar conclusions were also obtained with an SBS polymer modified bitumen [18]. The reduction in oxidation in both cases was attributed to the high aspect ratio of the OMMT silicate layers effectively reducing oxygen permeability (increased path length) and possibly obstructing the loss of volatile components from the bitumen at high temperature. In another investigation, organophilic clay (produced by ion exchange of hydrophilic clay with an organic cation, i.e. quaternary ammonium salt with alkyl chains) was pre-blended with a styrene-ethylene-butadiene-styrene block copolymer (SEBS) prior to bitumen modification, resulting in a reduction in phase angle, an increase in resistance to oxidative ageing, and interestingly an increase in high-temperature storage stability (attributed to the decrease in density difference between the SEBS and the dominant bitumen phases) [6].

With a focus on high temperature bitumen performance, this investigation was an ideal opportunity to put one or two ultra-fine filler/bitumen blends to the test. The 60/70 pen introduced in Fig. 7 was thus used as the base bitumen for all filler-bitumen blends. As a rough target, the aim was to produce at least one filler modified 60/70 pen bitumen that has a viscosity profile that was at least comparable to the next grade up, i.e. a 40/50 pen. The filler modified bitumen was next to be compared performance wise to the 40/50 pen using the MSCR test regime.

The first type of filler tested was calcium carbonate based, manufactured from high purity white marble, sourced from (Idwala Carbonates, Port Shepstone, South Africa). Samples were obtained from a portfolio of calcium carbonate fillers (product line brand name: KuluCote) routinely used as filler/pigment in the plastics and paint industry. A number of KuluCote filler samples were trialled having mean particle sizes ranging from 45μm down to 0.8μm. Furthermore, some of the selected filler samples had been pre-treated with a fatty acid (stearic acid) coating for enhanced dispersion.

The second filler type used was an organically modified bentonite clay (trade name: Falgel ED, manufactured by Falcon Technologies Inc., South Africa). The material is a nano-fine off white powder, with a specific gravity 1.6-1.8 g/cm^3. The powder is normally activated (e.g. using Methanol/water ratio of 95/5) prior to incorporation in final product. Typical applications include paints and inks. No other product information was made available. In this investigation, the Falgel following oven drying, was high shear blended directly with the bitumen without activating.

4.2 Preparation, testing and selection of optimized filler-bitumen blends

Blending the filler into the 60/70pen bitumen was carried out on a hot plate using a high shear mixer (5000 rpm at 130°C). Typically 0.5kg of bitumen was used per blend and blending times were around 40 minutes with filler being gradually introduced. The amount of filler required was calculated on volume basis and hence a 20% filler blend implies 20% filler addition by volume of bitumen.

The first task conducted following blending was to assess the storage stability in bitumen of the filler samples obtained. This was to ensure that any subsequent rheological measurements of the filler-bitumen blends were conducted on homogenous samples and the risk of filler settlement during testing was negligible.

The bitumen-filler blends (for all samples, 20% filler by volume of bitumen was selected for storage stability testing) were poured into glass test tubes 30 cm in length and these were then placed in an oven set at 160°C for 8 hours. At the conclusion of the 8 hours storage period, the test tubes were transferred to a freezer and subsequently the upper and lower quarters of the frozen sample were sliced off and the binder removed for further testing. A simple technique of dissolving the upper and lower bitumen/filler slices in toluene and passing the cold solution through a (Millipore – Fluoropore^{TM} Membrane Filters, 0.2µm) was used to determine the mass of filler in each binder slice. Based on this simple test, only three of calcium carbonate filler grades (belonging to the KuluCote family) investigated were classified as non-settling, and all remaining filler grades were discarded.

The largest high temperature storage stable mean filler size was found to be 2.3µm (stearic acid coated). Interestingly the 2.3µm “uncoated” filler did settle during the test. The two remaining non-settling fillers both had mean particle sizes of 0.8µm (one of which had stearic acid surface treatment, whilst the other had none).

Basic rheological analysis using DSR frequency sweeps were next conducted on the storage stable filler-bitumen blends. The next section describes the effect of varying the filler content and shear rate on complex viscosity. To maintain brevity, only the results from one KuluCote filler (0.8µm stearic acid coated calcium carbonate) are presented.

4.3 Investigating the effect of filler content on blend viscosity

The viscosity of a suspension is known to increase sharply with flocculation, in part due to the relative immobilization of a fraction of the suspended particles trapped in the agglomerates. Also at high concentrations of the solid phase, the existence of a velocity gradient results in rotation of the particles, followed by an increase in the viscosity of the suspension. This increase in viscosity is clearly demonstrated in Fig. 8, which is a plot of relative viscosity at 55°C as a function of filler fraction at various KuluCote (0.8µm size, stearic acid coated) volume fractions.

Examining a typical viscosity versus shear rate curve for the unfilled 60/70pen bitumen at 55°C as shown in Fig. 9, it can be seen that at exceedingly small shear rates, the material is essentially Newtonian in flow behaviour with a constant apparent viscosity, i.e. zero-shear viscosity (η_0). In the medium shear rate range, the apparent viscosity η begins to decrease, depicting typical shear thinning characteristic until it stabilizes to constant value (η_∞) at a considerably high shear rate in the upper Newtonian region (beyond the range of DSR used in this investigation).

Concentrated suspensions are known to exhibit non-Newtonian behaviour (as shown in Fig. 9) and hence viscosity would change as the shear rate (velocity gradient) changes. It is generally assumed that the viscosity dependence on shear rate is due to some structural changes in the suspensions such as the breaking up of agglomerates during shear. A suspension deflocculated by shear does not recover its structure immediately after the removal of shear since the thermal energy of the particles is insufficient to overcome the energy barrier for the flocculation [12].

As KuluCote filler content increases, Fig. 9 shows how the behaviour changes from Newtonian flow to pseudo-plastic flow with a yield stress σ_y. At low volume fractions, the yield value is negligible, however at moderately high volume fractions (30% in this investigation), the yield value is higher. Fig. 10 shows a log-log plot of shear stress as a function of shear rate at 55°C. It is interesting to compare the gradual change in the slope of the stress-rate curve as filler content increase in comparison to an almost perfect Newtonian behaviour of the 60/70pen at 70°C. The flow of Kulu-bitumen blends can be conveniently described by a Herschel-Bulkley [7] relationship designed for describing pseudoplastic fluids with yield stress as follows:

$$\sigma = \sigma_y + k\dot{\gamma}^n \qquad ...(8)$$

where; k and n are the consistency factor and the power law index respectively.

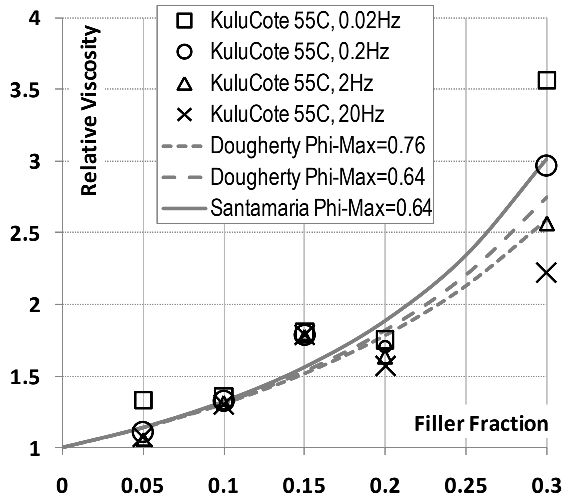

Figure 8: Plots of relative viscosity as a function of shear rate for various filler volume fractions.

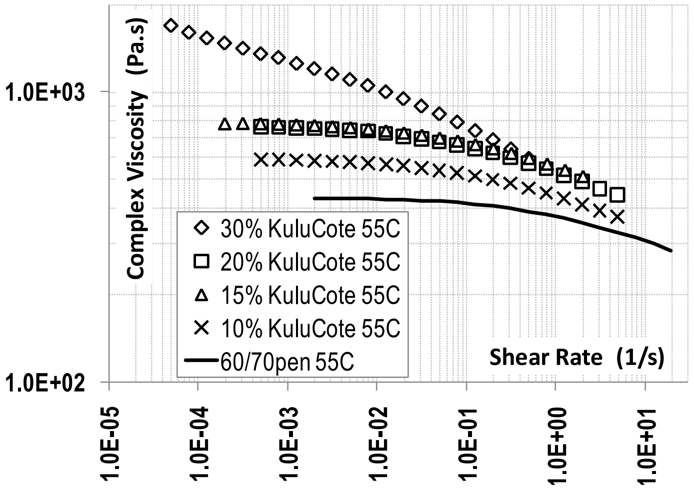

Figure 9: DSR complex viscosity versus shear rate for various filler-bitumen proportions.

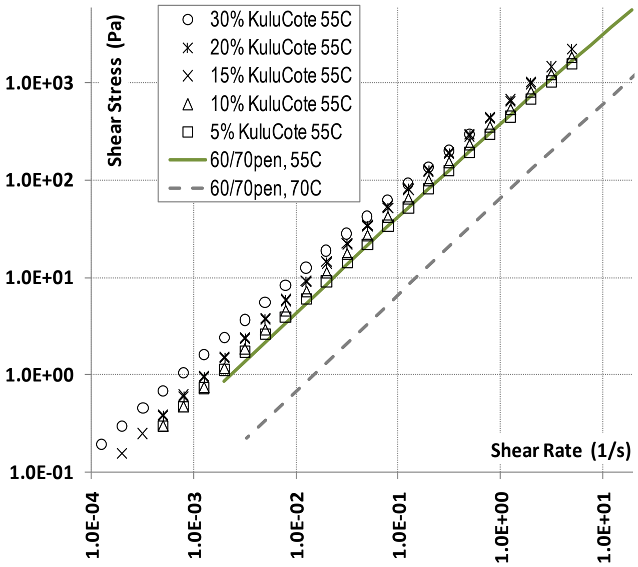

Figure 10: log-log plots of shear stress as a function of shear rate for the various filler volume fractions.

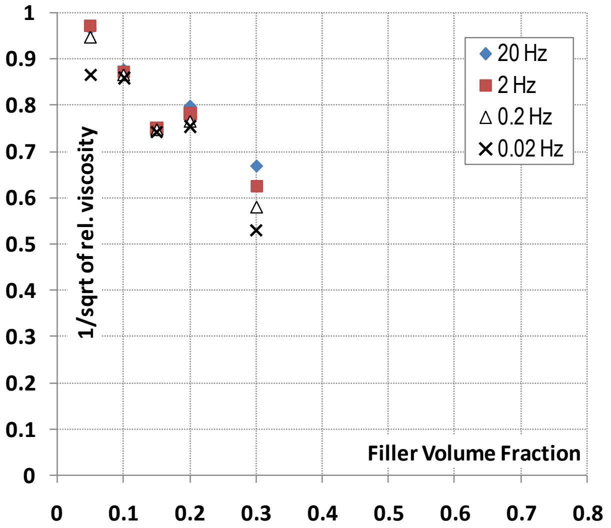

Figure 11: Graphical method for approximating maximum packing of filler.

A commonly used semi-empirical formula to interpret the relative viscosity of suspensions incorporating hard-sphere systems is the Krieger-Dougherty relation, which has the following form [1]:

$$\frac{\eta_s}{\eta} = \left(1 - \frac{\phi_V^*}{\phi_{max}}\right)^{-2.5\phi_{max}} \qquad ...(9)$$

where: η_s = dynamic viscosity of a suspension, η = dynamic viscosity of suspending fluid, ϕ^*_V = effective hydrodynamic volume of particles (which is larger than volume of particles in the dry state), ϕ_{max} = maximum packing fraction of particles, estimates for monodisperse suspensions $\phi_{max} \approx 0.64$ (random close packing of identical spheres) whilst for polydisperse suspensions characterised by a broad size distribution $\phi_{max} \approx 0.76$.

More recent work has developed the following expression in the case of hard-spheres with $\phi_c = 0.64$ [10]:

$$\frac{\eta_s}{\eta} = \left(1 - \frac{\phi}{0.637}\right)^{-2}\left[1 - 0.64\phi + 0.415\phi^2\right] \qquad ...(11)$$

where: ϕ = volume fraction, ϕ_c = critical concentration at which the suspension loses its fluidity, which is generally greater than the purely geometrical percolation threshold of the particles but less than or equal to the maximum packing fraction ϕ_{max}.

Maximum packing fraction can in theory be estimated, by plotting $\eta_r^{-0.5}$ against filler volume fraction (ϕ_{eff}) and extrapolating to zero [7]. A rough attempt at estimating ϕ_{eff} is shown in Fig. 11 which had the added complication that the viscosity data were generated from dynamic as opposed to steady state shear flow measurements and this has created more than one possible extrapolated solution (range from 0.7 to just below 0.8). Nonetheless, one can clearly see the usefulness of this approach.

Deviations from Eq. 9 and Eq. 10 in Fig. 8 have also been attributed to electrostatic interactions connected with the presence of fixed charges at particle surfaces causing the maximum packing of particles to become smaller than the hard sphere value ϕ_{max}. In the presence of shearing flows the electrostatic effects increase the energy dissipation in particle suspensions that results in increased viscosity. It is expected that the repulsive electrostatic interactions among particles will play an even more pronounced role for the higher concentration range of the suspension [1].

4.4 Selection of best performing filler-bitumen blends

In order to narrow down the selection process to the best performing calcium carbonate filler, filler-bitumen blends were next manufactured from each of the (KuluCote range) calcium carbonate fillers at 10%, 20% and 30% by volume of bitumen. Rheological characterisations were carried out using a DSR by initially conducting strain sweeps to determine the linear viscoelastic (LVE) strain regions. The test temperatures selected were 20, 40, 55 and 70°C. At each temperature a maximum allowable dynamic strain value was established which allowed frequency sweeps to be conducted within the LVE range at each test temperature. The results from frequency sweeps were subsequently combined into Black diagrams (e.g. Figs. 12 & 13). Selection of the best performing calcium carbonate filler was carried out by examination of the Black diagram plots and identifying the filler type resulting in the least amount of deviation from the thermo-rheologically simple 60/70pen. curves. The best performing calcium carbonate filler was thus found to be KuluCote95T (henceforth referred to as KuluCote), the main properties of which are shown in Table 2.

Table 2: Composition of best performing KuluCote calcium carbonate filler

$CaCO_3$ = 96.5%	Residue on 45μm sieve = 0.008%
$MgCO_3$ = 2.8%	Top cut (d98%) = 5μm
Fe_2O_3 = 0.03%	Mean particle size (d50%) = 0.8μm
Acid insoluble content = 0.5%	Particle < 2μm = 86%
Fatty acid treatment = 1.2%	Relative density = 2.7 g/ml

Figs. 12 and 13 focus on the performance of KuluCote filler-bitumen blends (10%, 20% and 30% by volume) in comparison to the 60/70 pen base bitumen. It would be expected that following blending with filler, the stiffening/reinforcing action would cause the phase angle values (δ) of the KuluCote blends to shift towards lower values compared to the original 60/70 pen at all temperatures.

Examining the frequency sweeps at 20°C in Fig. 12 show clear reductions in phase angles as the KuluCote content is increased and this reduction is magnified as the rate of loading is reduced (as one moves down a particular curve). At 40°C and 55°C, the 10% and 20% blends were more in line with the 60/70 pen performance with a progressive reduction in δ values, whilst at 30% filler content, a major deviation is observed.

As this study is focused on assessing high temperature performance, the behaviour at 70°C was of most interest. It was particularly evident in Fig. 13 that at 30% filler and 70°C test temperature, the behaviour was far more erratic. All the viscoelastic, rheologically simple behaviour anticipated from a pen grade bitumen was lost across the entire frequency spectrum. It must be reiterated at this point that the other (larger particle sized) KuluCote-type fillers black diagrams (not shown in this paper) were even more erratic and unpredictable compared to the current sample and as discussed earlier, this was a primary method of selecting the best performing KuluCote filler.

Focusing on the 70°C performance, a plot of complex viscosity η* versus frequency is shown in Fig. 14. A KuluCote addition of 20% by volume, changes the bitumen performance by approximately one grade (e.g. from 60/70 pen to 40/50 pen). Taking an overview of all the results, an upper working limit, that guarantees homogeneity and no structuring, for KuluCote-bitumen blends can be set at a maximum of 20% (by volume). Beyond 20% the risk of agglomerations, structuring and colloidal instability, dramatically reduce the possibility of a consistent homogeneous mastic that can be rheologically characterised with any degree of confidence.

Falgel contents (by volume of bitumen) were also tested at 2%, 3%, 4%, and 5%. Figs. 16 and 17 show black diagrams of the Falgel-bitumen blends at 2%, 3% and 4%. The 5% blend produced completely unpredictable Black diagrams, with test results that were not repeatable, and was hence discarded. Fig. 15 shows a viscosity-frequency plot for the Falgel-bitumen blends compared to the base bitumen and the 40/50 pen. Taking an overview of Figs. 12 to 17 shows that only 3% Falgel blended into a 60/70pen grade bitumen will produce a binder that is slightly stiffer than (considering phase angle and complex viscosity) the 20% KuluCote blend.

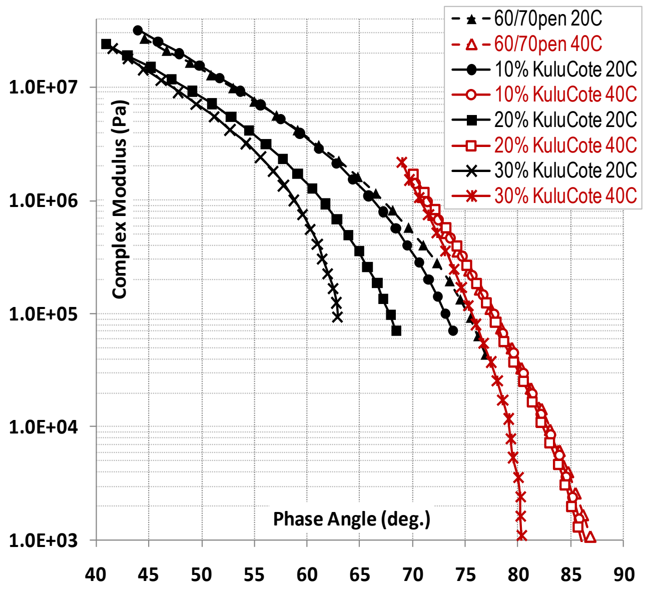

Figure 12: Black diagrams of best performing carbonate (KuluCote) filler at 20°C & 40°C

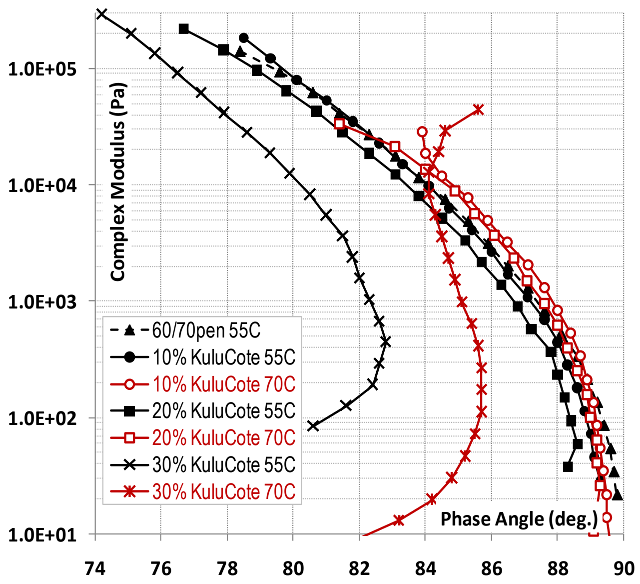

Figure 13: Black diagrams of best performing carbonate (KuluCote) filler at 55°C & 70°C.

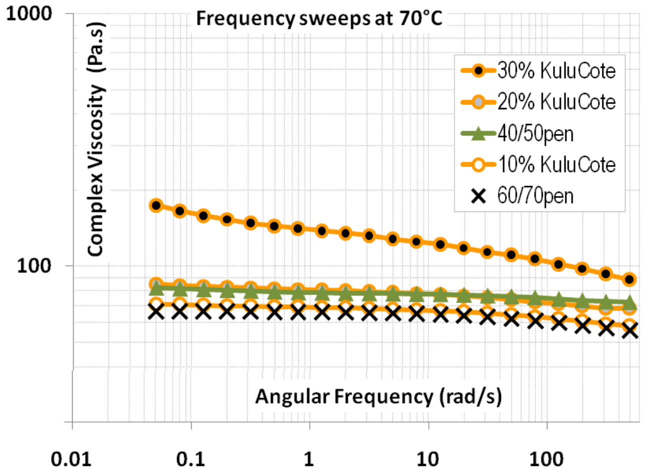

Figure 14: Viscosity versus frequency trend lines of carbonate (KuluCote) filler-bitumen blends.

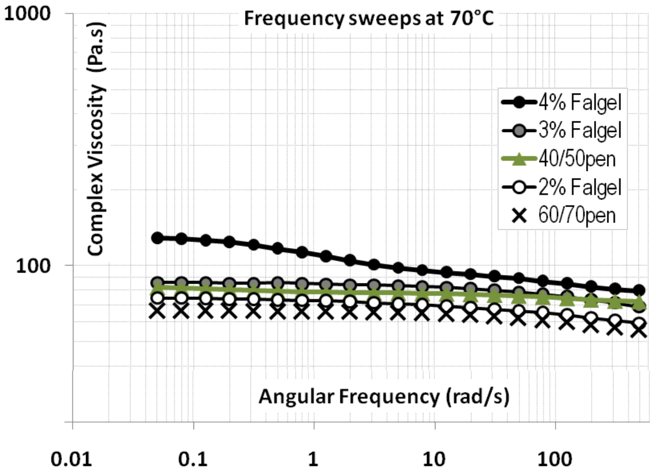

Figure 15: Viscosity versus frequency trend lines of bentonite clay (Falgel) filler-bitumen blends.

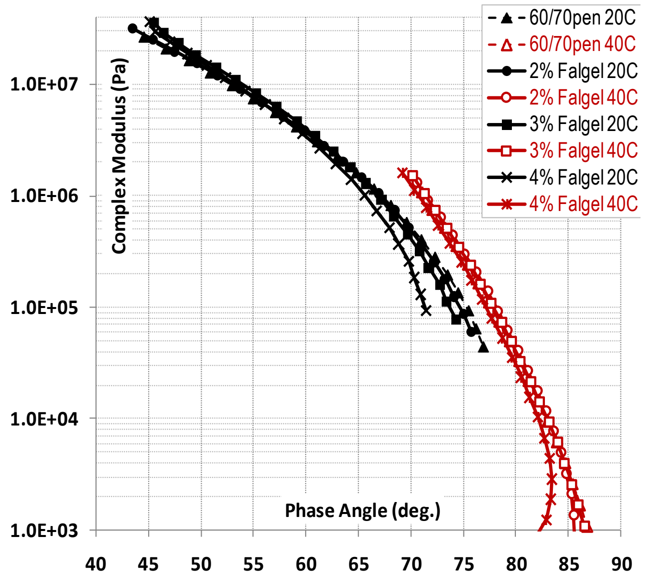

Figure 16: Black diagrams of bentonite clay (Falgel) filler at 20°C & 40°C.

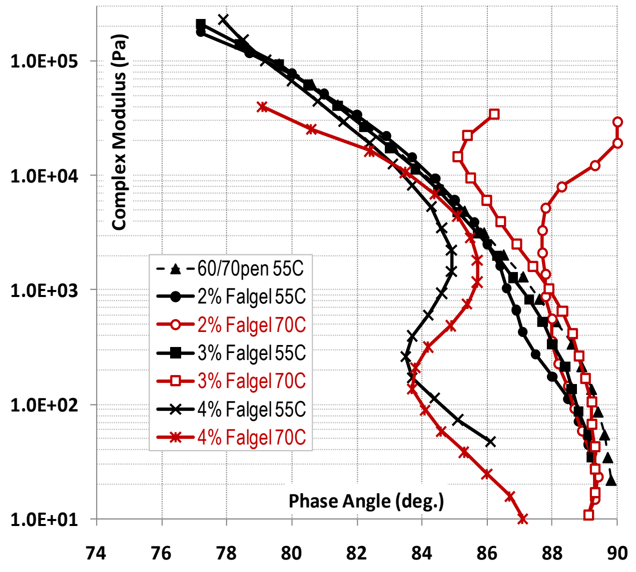

Figure 17: Black diagrams of bentonite clay (Falgel) filler at 55°C & 70°C.

5. Comparison of MSCR testing of all Bitumens at 70°C

Fig. 18 shows a plot of the % non-recoverable compliance (J_{nr}) versus applied stress obtained from MSCR tests at 70°C for selected bitumen samples as described in Sections 3 & 4. The most striking evidence from the Figure is the seemingly superior performance of the SBS modified binder at 70°C in comparison to all other straight run and filler-bitumen blends. At the same time, the SBS binder happens to be the most stress sensitive, with the binder completely breaking down beyond around 3200 Pa. It is also remarkable to note that the straight run 20/30 pen is substantially more stress resilient than the SBS binder at the same test temperature, and that the 40/50 pen, though having completely inferior J_{nr} ranking, has a very similar stress sensitivity threshold to the 20/30 pen.

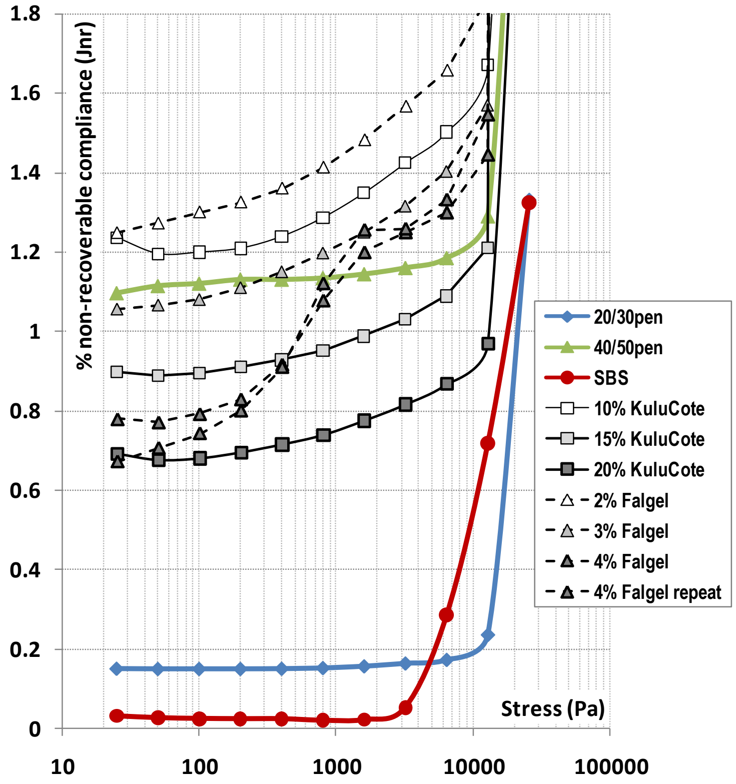

Figure 18: Non recoverable creep compliance (%J_{nr}) obtained from MSCR tests at 70°C

The performance of the filler-bitumen blends was in agreement with their complex viscosity or phase angle rankings, with higher filler contents resulting in reduced J_{nr}. It is also clear that despite having very different J_{nr} versus stress profiles, all the filler-bitumen blends retained the same failure stress level (around 12800 Pa) in line with the two other pen grade bitumens. Comparing the two filler types, it is clear that the Falgel blends were far more sensitive to increasing stress compared to the KuluCote blends.

It was discussed earlier using viscosity-frequency profiles at 70°C (Figs. 14 and 15) that modifying a 60/70 pen with either 20%KuluCote or 3%Falgel would result in a binder with performance close to a 40/50pen, it was therefore of great interest to compare these three "viscosity-comparable" binders. The 20%KuluCote blend was superior in all aspects to its viscosity-comparable Falgel blend. Nonetheless, it is fascinating how much rheological modification can be imparted on a bitumen with only 3-4% nano-fine filler. The completely different stress sensitivity profile of the 4% Falgel blend (a repeat test is shown in Fig. 18 to indicate that such a steep profile is not caused by experimental error) emphasises that before one can dismiss the performance of such an ultra-fine filler, a better understanding of what stress levels are realistically expected from bitumen films in an asphalt composite under vehicular traffic loading at high temperatures.

One can crudely conclude at this stage that varying the pen grade of unmodified bitumens does not result in a dramatic effect on the MSCR failure stress levels. Artificially increasing the binder viscosity or stiffness by blending in micro or nano-sized fillers affects the stress sensitivity but not the actual value of ultimate failure stress, which remains in line with the base bitumen. On the other hand, elastomer modification completely alters the failure stress criteria.

6. Conclusions

The Arrhenius relation was found to be perfectly adequate for characterising the temperature dependency of viscosity of a typical straight run bitumen, especially at high temperatures. On the other hand, the SBS modified bitumen tested in this investigation showed that the Arrhenius treatment was completely inadequate at characterising a non thermo-rheologically simple bitumens.

When considering the SBS modified bitumen tested in this investigation, the concepts of zero and low shear viscosity were found to be not readily applicable as no viscosity plateau can be observed at very low shear rates. The multiple stress creep recovery (MSCR) test methodology, in particular when conducted at a single test temperature, was more capable of characterising and ranking the high temperature performance of all the bitumen types trialled in this investigation.

Rheological modification of a straight run bitumen using simple high shear blending with either micro-sized calcium carbonate or nano-sized clay fillers was shown to be very viable. The filler-bitumen storage-stable bitumen blends demonstrated enhanced MSCR high temperature performance.

The downside to incorporating ultra fine fillers was the increased difficulty of interpreting DSR derived complex modulus versus phase angle (Black diagrams) as the filler content is increased. Increased filler content is also accompanied by rapid deviation from thermo-rheologic simplicity. Furthermore, different filler types presented very different stress sensitivity behaviour during MSCR testing.

The manufacturing process of storage-stable ultra-fine filler-bitumen blends is relatively straight forward and may be conducted at will by a contractor as opposed to relying on the bitumen supplier. The fillers are relatively easily sourced and it is thus very worthwhile investigating the economics of such additive operations.

References

1. Adamczyk Z., Jachimska B. and Kolasinska M., “Structure of colloid silica determined by viscosity measurements”, Journal of Colloid and Interface Sciences, 273 (2004) 66/-674.
2. Binard C., Anderson D., Lapalu L., Planche JP. (2004), “Zero Shear Viscosity of Modified and Unmodified Binders”, 3rd Eurasphalt & Eurobitume Congress, Vienna, Book 2, pp. 1721-1733.
3. D’Angelo J. and Dongre Raj, 2009. *Practical use of Multiple Stress Creep and Recovery Test*. Transportation Research Record, Journal of the Transportation Research Board, No. 2126, pp. 73-82.
4. Giuliani F. and Merusi F. (2008), “Experimental evaluation of asphalt binders high specification temperature based on the low shear viscosity concept”, 4th Eurasphalt Eurobitume Congress, Session 4, paper no. 402-054.
5. Guericke R. and Schlame K. (2008), “A new softening-point based on asphalt pavement performance figures”, 4th Eurasphalt & Eurobitume Congress, Copenhagen, paper no. 402-089.
6. Jahromi S.G. and Khodaii A., “Effects of nanoclay on rheological properties of bitumen binder”, Construction and Building Materials 23 (2009) 2894-2904.
7. Luckham P.F. and Ukeje M.A. “Effect of particle size distribution on the rheology of dispersed systems”, Journal of Colloid & Interface Science 220, 347-356 (1999).
8. Mturi G.A.J. and Zoorob S.E., “Effect of shear rate on bitumen viscosity measurements, relevance to high temperature processing of bituminous products”, 10th Conference on Asphalt Pavements for Southern Africa (CAPSA11), 11-14 Sept. 2011, KwaZulu Natal, South Africa.
9. NCHRP 1-37A, 2004, Transport Research Board, Guide for Mechanistic-Empirical Design of New and Rehabilitated Pavement Structures, Part 2: Design Inputs, Chapter 2: Material Characterization.
10. Petersen J.C. et. al., Strategic Highway Research Program, SHRP-A-370, 1994, Binder Characterization and Evaluation, Volume 4: Test Methods, Chapter 1: Dynamic Shear Rheometry. ISBN 0-309-05806-6.
11. Santamaria-Holek I. and Mendoza C.I., “The rheology of concentrated suspensions of arbitrarily shaped particles”, Journal of Colloid and Interface Science, 346 (2010) 118-126.
12. Shenoy AV. Rheology of Filled Polymer Systems, Kluwer Academic Publishers; 1999, ISBN 0-412-83100-7.
13. U.S. Asphalt Institute Guidance Document, April 2010. *Implementation of the Multiple Stress Creep Recovery Test and Specification*.
14. Van Rooijen RC. and de Bondt AH. (2004), “Experience with the zero-shear viscosity concept to characterise rutting”, 3rd Eurasphalt & Eurobitume Congress Vienna, Book 2, pp. 1588-1598.
15. Visscher J.De and Vanelstraete A. (2009), “Equiviscous temperature based on Low Shear Viscosity, evaluation as binder indicator for rutting and critical discussion of the test procedure”, Advanced Testing and Characterization of Bituminous Materials, Loizos, Partl, Scarpas & Al-Qadi (eds), ISBN 978-0-415-55854-9, pp. 1009-1018.
16. Ward IM. Mechanical Properties of Solid Polymers. 2nd ed. 1979, John Wiley & Sons, ISBN 0-471-90011-7.
17. Yu J.Y., Feng P.C., Zhang H.L. and Wu S.P., “Effect of organo-montmorillonite on aging properties of asphalt”, Construction and Building Materials 23 (2009) 2636-2640.
18. Zhang H., Yu J., Wang H. and Xue L., “Investigation of microstructures and ultraviolet aging properties of organo-montmorillonite/SBS modified bitumen”, Journal Materials Chemistry and Physics, April 2011.
19. Zoorob S.E. Castro-Gomes J.P. and Pereira-Oliveira L.A., “Assessing Low Shear Viscosity as the New Bitumen Softening Point Test”, accepted 18th July 2011, Construction & Building Materials, Elsevier.